Nuclear Science & Technology Research Institute

Journal of Nuclear Research and Applications

Research Paper

Journal homepage: https://jonra.nstri.ir

Feasibility of Anthropomorphic Head Phantom Design Using DLP 3D Printing for Dosimetry

A. R. Khoshhal*, A. Esmaili Torshabi

Nuclear Engineering Group, Faculty of Sciences and Modern Technologies, Graduate University of Advanced Technology, P.O.Box: 7631885356, Kerman, Iran.

(Received: 4 August 2024, Revised: 28 August 2024, Accepted: 8 September 2024)

A B S T R A C T

Despite the increasing expansion of radiation therapy and diagnostic radiation centers in the country aimed at improving the quality of treatment for various diseases, challenges such as dosimetry, calibration, and quality control of radiation therapy and diagnostic devices still persist. In this sense, preparing and making a suitable phantom is important. Phantoms are used in dosimetry due to their density and effective atomic number similar to body tissues. Among the phantoms prepared for dosimetry purposes is the Rando phantom. The main purpose of this study is to determine the feasibility of the materials for making the anthropomorphic head phantom (AHP) head and neck phantom using a Digital Light Processing (DLP) 3D printer, as well as the design of the whole human body phantom with the lowest cost. The dimensions of different parts of the phantom were extracted from CT-Scan images and were designed using SolidWorks, Meshmixer, and Ultimaker Cura. In this study, the use of Thermoplastic Polyurethane (TPU) resin, equivalent to soft tissue and bone tissue, was evaluated. Considering that the density of soft tissue and skull bone is 1 $^{gr}/_{cm^3}$ and 1.6-1.7 $^{gr}/_{cm^3}$, the density of these two resins is 1 $^{gr}/_{cm^3}$ and 1.6 $^{gr}/_{cm^3}$. In order to verify the accuracy of our developped phanom a Monte Carlo based simulation assessment was done using GEANT4 code. The final results indicate good agreement between our phantom and other commonly available phantoms.

Keywords: Anthropomorphic phantom; 3D printer; Internal dosimetry; Monte carlo simulation.

1. Introductions

Phantom is a numerical and physical model that simulates the characteristics of various human anatomical structures. Phantoms are widely used for dosimetry, as well as for the calibration and quality control of radiation therapy devices. In internal dosimetry, the unavailability of internal organs and tissues, along with the presence of various types of

*Corresponding Author E-mail: amirrezakhoshhal79@gmail.com

DOI: https://doi.org/10.24200/jonra.2024.1634.1140.

radiations, makes practical dosimetry challenging. Direct placement of a detector inside the desired organ or tissue is not feasible. During radiation therapy with any radiation, it is crucial to prevent normal tissues from absorbing an excessive dose.. On the other hand, Measuring and evaluating the absorbed dose is critical is an important issue. Therefore, creating a new phantom model can be highly beneficial for accurate dose calculation prior to actual treatment [1]. In this context, the development of an appropriate phantom is essential. External beam radiation therapy, a standard cancer treatment, is used to deliver targeted radiation to known tumor sites. However, its effectiveness is often limited by the toxicity to normal tissues that are anatomically close to the tumor. In head and neck cancer, the tumor is frequently located near critical structures critical structures such as the spinal cord, brainstem, and visual organs [2].

Radiation therapy plays a crucial role in the treatment of head and neck cancer with offering a high probability of tumor control with a low risk of complications to normal tissues. In image-guided radiotherapy of the head and neck absorbed doses to vital organs such as the lens, parotid gland, and thyroid gland are of concern; because they have already received doses from the course of radiotherapy. Phantoms are used to measure the absorbed dose during the treatment process and help prevent excess radiation exposure to sensitive tissues [3]. Phantoms are used in dosimetry due to their density and effective atomic number closely resemble those of human tissues. One of the phantoms prepared for dosimetry purposes is Rando phantom. The head phantom allows us to place dosimeters of various sizes dosimeters in many locations of the phantom volume. The human head exhibits heterogeneous characteristics with distinct dielectric properties of head tissues attributed to varying components such as water, fat and protein. Due to the distinctive characteristics of head tissues, researchers have developed various categories of head phantoms for imaging purposes. Examples include a heterogeneous phantom, a 3D printed phantom, a four-shell diffusion phantom, a plaster phantom, a reconfigurable phantom, and a head-sized phantom. The fabricated head phantom enables us to place dosimeters of different sizes in various locations within the phantom volume. The head phantom is created using three-dimensional arrangements filled with numerous biochemical compounds, whose density and effective atomic number are similar to that of body tissue.

Today, various imaging technologies are used in the medical research system to diagnose brain abnormalities in the human head. These technologies include computed tomography scanning, magnetic resonance imaging, X-ray mammography, ultrasound, and positron emission tomography. Low energy photons can be harmful to human organs, tissues, and DNA. Significant phantom materials that can be used in diagnostic radiology, radiation protection, radiation dosimetry, and dose estimation were reviewed for their essential radiation application values. The interaction of gamma-ray photons with matter has always been a field of great interest among researchers due to its usefulness in medical imaging, radiation therapy, energy production, and food science. A thorough understanding of these interactions is

necessary to accurately measure and control gamma radiation in various applications in order to minimize the risks of exposure and maximize their benefits [4]. Fuquan Zhang et al in their study, fabricated a lung phantom using a 3D printer. The phantom was created based on anonymized human chest CT images and consisted of a 3D-printed skin shell, filled with tissue-equivalent materials that had similar radiation attenuation characteristics. The filling materials included a mixture of $CaCO_3$, MgO, agarose, NaCl, pearl powder and silica gel [5]. In a study by Matthew M. Mille et al, they demonstrated an on-demand and nearly automatic method for fabricating tissue-equivalent physical anthropomorphic phantoms for imaging and dosimetry applications. This was achieved using a dual nozzle thermoplastic three-dimensional (3D) printer and two types of plastic. The printed phantom included 30 separate anatomical regions, such as soft tissue remainder, lungs, heart, esophagus, rib cage, clavicles, scapulae, and thoracic vertebrae [6]. Nikiforos Okkalidis investigated various 3D printing methods for radiological anthropomorphic phantoms. Five main types of 3D printing methods have been explored: (a) solidification of photo-curing materials; (b) deposition of melted plastic materials; (c) printing paper-based phantoms with radiopaque ink; (d) melting or binding plastic powder; and (e) bio-printing [7].

Low-energy photons are widely used in the medical field for various purposes such as medical imaging, radiography, and radiotherapy, as well as for radiation protection, radiation dosimetry, and dose estimation. Therefore, understanding their interactions is essential because low-energy photons are more damaging than high-energy photons. Phantom materials are artificial materials designed to mimic human tissues and have values of mass attenuation coefficients and effective atomic number similar to real human tissues. These can be made of various materials such as polymers, gels, plastics and even real tissue. In the research by Josefine Cederhag et al., their purpose was to establish the correlation between thermoluminescence dosimeters (TLDs) and Gafchromic film to measure absorbed doses and compare the minimum, maximum and average absorbed doses in larger areas of interest and in different organs and tissues of the skull during cone beam computed tomography (CBCT). The result of their work was that TLD positioning could not cover several organ sites, therefore only measurements of the absorbed dose from the film were available [8]. The aim of the study by Durer Iskanderani et al. was to map and compare the distribution of absorbed doses using Gaffochromic film for panoramic radiography and cone beam CT scans (CBCT) of the temporomandibular joint (TMJ) in both adults and children. The results of their work showed that the absorbed doses varied significantly among different radiosensitive tissues. In both panoramic and CBCT examinations of the TMJ, the bone surface and salivary glands received the highest absorbed doses compared to other tissues [9]. Although there are various reports on creating phantoms using different 3D printers, including fused deposition modeling 3D printers and various materials [10,11].

In our opinion, these methods have flaws such as the presence of holes, non-uniformity of

the produced product, long manufacturing time and high cost. Therefore, we explored the possibility of using a DLP 3D printer with TUP resins which are readily available and inexpensive to create this phantom. In addition to this, we looked into factors such as cost reduction, construction time, and design accuracy, making significant progress. Our results closely match the real results. In this study, we initially used the GEANT4 simulation code to compare soft tissue and bone tissue with resins in terms of factors like density and effective atomic number. We then utilized CT-scan images and GEANT 4 to extract the exact dimensions of the skull . We designed the skull using Meshmixer, Ultimaker Cura, and Solid Works software and analyzed the results.

3. Experimental

3.1. GEANT4 simulation code

In the research the GEANT4 toolkit was used as a Monte Carlo simulation tool that can simulate the passage of particles through matter. Its applications include high energy, nuclear, and accelerator physics, as well as studies in medical and space science. GEANT 4 simulates the interaction between particles and matter.

GEANT4 provides a series of tools to describe complex geometry and material properties of an experimental setupIt covers various categories of physics that handle particle transport through detector elements. it can be used in the energy region from one eV to 10^{12} eV energy allowing for the management of real conditions, physical models and geometry to approach experimental conditions. Therefore, GEANT4 is considered to be more accurate than other similar simulation packages.

GEANT4 is written in C++, which enables microscopic simulations of the propagation of particle interactions with materials. This simulation toolkit is widely used in areas such as medical physics, gamma-ray shielding and high-energy physics experiments [12,13]. The GEANT4 modeling flowchart is shown in Fig. 1.

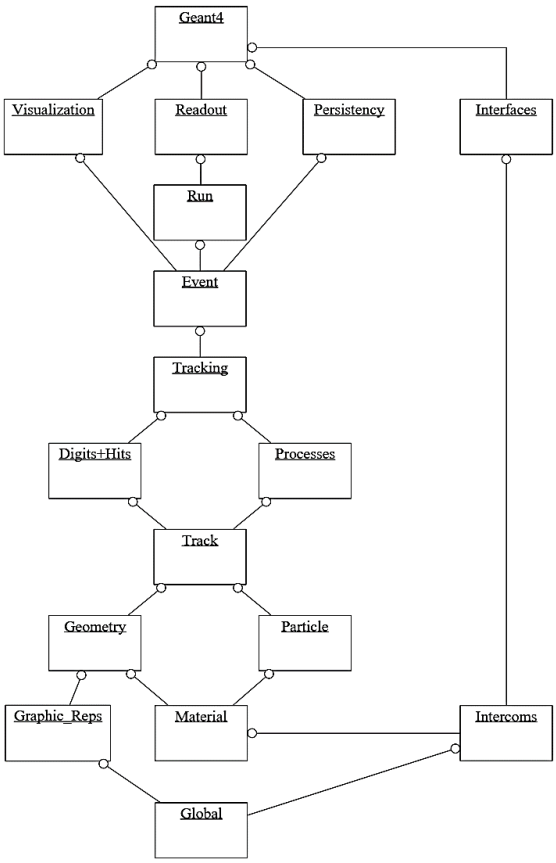

Fig. 1. The GEANT4 modeling flowchart [14].

In the first part of this research, target volume was defined using the Monte Carlo method and the GEANT 4 simulation code. The dimensions of the target were set at 5 cm × 5 cm × 3 cm, with of the detector measuring 25 cm^2. Initially, the target was defined as a combination of soft tissue and bone. The number of rays reaching the detector was then evaluated using a photon beam emission with a

width of 2 cm and the results of this assessment were recorded as a reference.

In the next stage of the study, the target volume was modified to include two TPU resins, which were considered to be equivalent to bone tissue and soft tissue. (Fig. 2.)

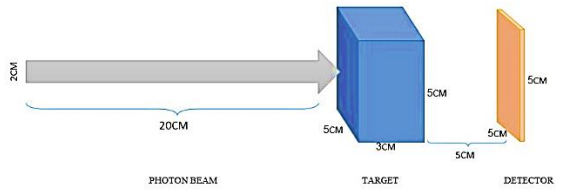

Fig. 2. The Photon Beam, Target volume and Detector.

In the following section, the dimensions of the target volume have been adjusted to 10cm × 10cm × 10 cm, with the detector measuring 100 cm^2. The components of this volume are defined as in the initial part: skull bone and soft tissue as a reference, followed by two TPU resins. Subsequently, the depth of penetration of a proton beam emission with a width of 2 cm into the target with various materials was examined. (Fig. 3.)

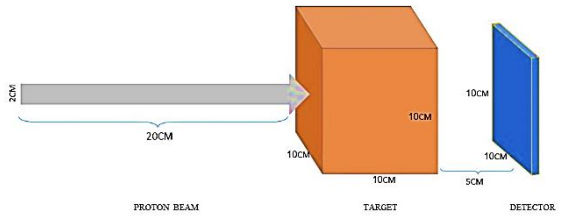

Fig. 3. The Proton Beam, Target volume and Detector.

In this simulation code, all the constituent elements of resins, soft tissue and bone tissue are defined. All physical and chemical properties as well as the most important factors such as density and effective atomic number related to them were applied.

3.2. DLP 3D printing

DLP is named after the digital light projector [15], which is based on digital micro-mirror device (DMD) technology [16]. The photosensitive resin is polymerized locally and forms a stack of layers through a back to-back projection of images of 2D layers from a DLP source. These images consist of light and dark pixels created by micron-sized mirrors on DMD, which determine the XY-plane resolution of the polymerized layer. This technology falls under the category of the vat polymerization process, along with stereolithography. It follows the same basic steps of manufacturing as other additive manufacturing (AM) technologies, which include designing, printing, and post processing.

A brief overview of the complete DLP process is depicted in the flowchart in Fig. 4. Pre printing steps may vary depending on the specific computer aided design (CAD) and slicing software being used. For example, some slicing software can generate support structures or fix critical issues in the .stl file, such as holes or intersections. In this study, taking into account the characteristics of 3D printers, such as product uniformity and absence of holes, it is anticipated that this method can be utilized to create phantoms.

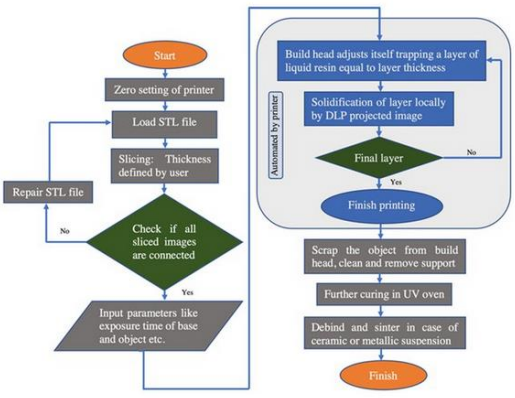

Fig. 4. Schematic flow diagram of a DLP printing process [17].

3.3. Phantom design

Here, we used head CT scan images to extract the desired phantom dimensions using GEANT4 code. We then designed the phantom using Ultimaker Cura, Meshmixer and Solid Works software. When designing the phantom from the outside to the inside we considered, the first layer, as the skin layer on the skull, the second layer as the skull bone and the inner soft tissue layer. (Fig. 5 and 6)

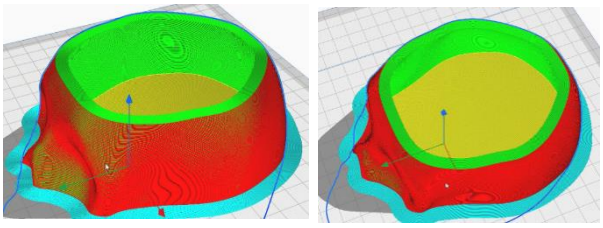

Fig. 5. Phantom design using Ultimaker Cura software (Red is Skin and equal to soft tissue, green is skull bone and yellow is soft tissue).

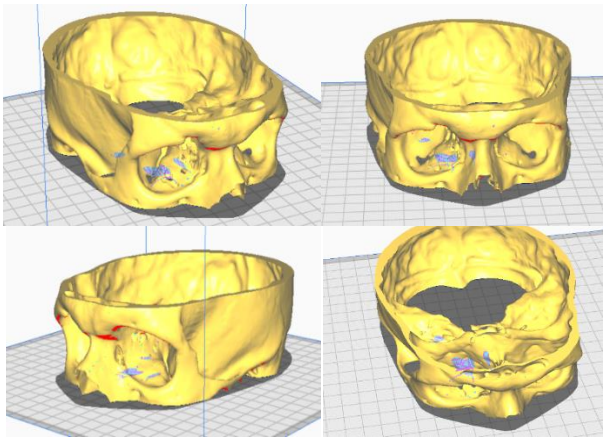

Fig. 6. skull design using Solid work and Meshmixer software.

In the final stage of the research, we explored the creation of the AHP phantom using a DLP 3D printer. The prototype was initially produced using a Fused Deposition Modeling (FDM) 3D printer as depicted in Fig. 7.

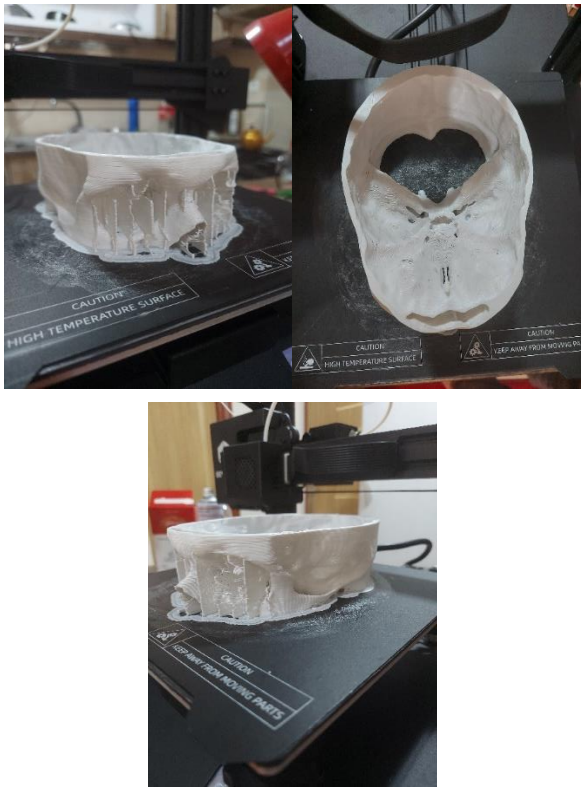

Fig. 7. Skull of AHD Prototype using FDM 3D printer.

4. Results and discussion

In the first part of the simulation using the GEANT4 code, the comparison of the number of particles that reached the detector after passing through the reference materials and two resins revealed that the use of two resins in this research is highly beneficial. Table 1 displays the results, showing that the two resins yield similar results to the reference materials.

According to Table 1, the percentage of particles that reached the detector in bone tissue and TPU resin is $54.59 \pm 1.25\%$ and $55.66 \pm 1.61\%$, respectively. Similarly, for soft tissue and TPU resin, the values are$66.60 \pm 1.13\%$ and $67.09 \pm 1.34\%$, respectively.

After examining the Bragg curve in Fig. 8 and the penetration depth of the particles in Fig. 9, the results indicate that the penetration depth of the proton beam in the two resins is nearly identical to the penetration depth in the reference tissues, as shown in Table 2. The table illustrates that the penetration depth in bone tissue and TPU resin is 55 ± 0.42 mm and 56 ± 0.52 mm, while the value for soft tissue and TPU resin is 77 ± 0.97 mm and 78 ± 1.1 mm.

Table 1. The percent of particles that reached to the detector.

	Skull bone (Density: 1.6 $^{gr}/_{cm^3}$)	TPU resin (Density: 1.6 $^{gr}/_{cm^3}$)	Soft Tissue (Density: 1 $^{gr}/_{cm^3}$)	TPU resin (Density: 1 $^{gr}/_{cm^3}$)
particles (%)	54.59 ± 1.25	55.66 ± 1.61	66.60 ± 1.13	67.09 ± 1.34
Code Error (%)	2.3	2.9	1.7	2.01

Table 2. The penetration depth of proton in tissues and resins.

	Skull bone (Density: 1.6 $^{gr}/_{cm^3}$)	TPU resin (Density: 1.6 $^{gr}/_{cm^3}$)	Soft Tissue (Density: 1 $^{gr}/_{cm^3}$)	TPU resin (Density: 1 $^{gr}/_{cm^3}$)
penetration depth (mm)	55 ± 0.42	56 ± 0.52	77 ± 0.97	78 ± 1.1
Code Error (%)	0.71	0.94	1.26	1.42

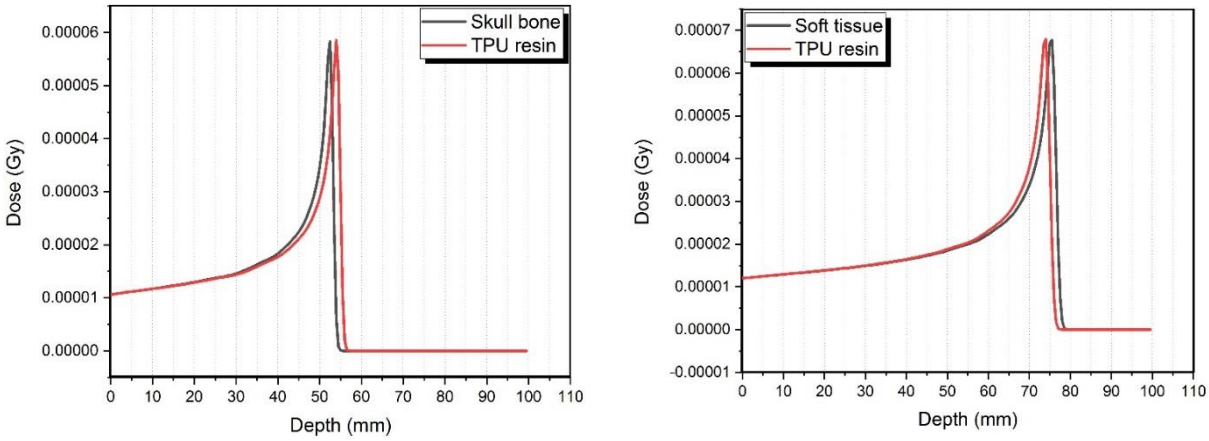

Fig. 8. The Bragg curve of results.

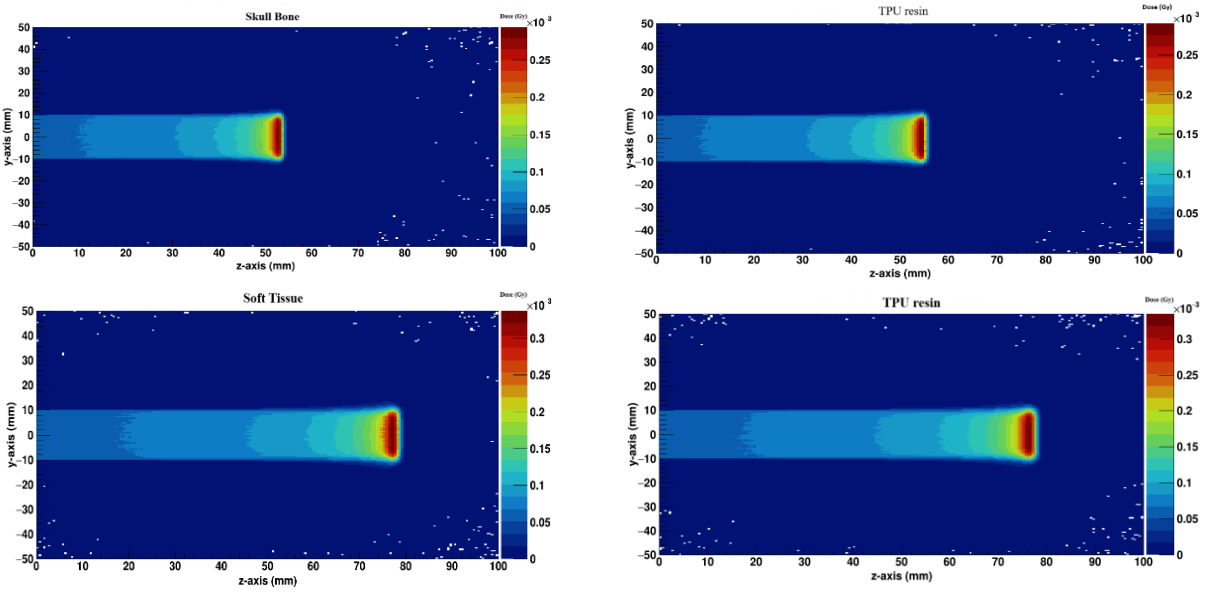

Fig. 9. Proton penetration depth in the target volume.

In future research following the development of this product, we will analyze the dosimetry results using the AHP phantom in comparison to a reference phantom (e.g. Rando phantom). Due to the fact that the density of lung tissue is 0.6 g/cm^3, we anticipate encountering limitations and challenges in creating this portion of the phantom.

5. Conclusions

Phantoms are anatomical structures that representthe whole human body and are utilized in dosimetry, quality control, and calibration of radiation therapy and diagnostic radiation devices. One method of creating phantoms is through the use of 3D printers. This research, the explores the feasibility of producing a phantom using a DLP 3D printer and TPU resins with varying densities. The necessary dimensions were obtained from CT scan images, and factors such as density and effective atomic number were incorporated into the GEANT4 simulation code.

The simulated volumes were the subjected to both photon beam and proton beam irradiation.The results indicate that the percentage of particles reaching the detector for bone and an equivalent TPU resin is 54.59% and 55.66%, respectively, showing only a 1.07% difference in the number of photons reaching the skull bone compared to the equivalent TPU resin. Similarly, for soft tissue and the equivalent TPU resin, the percentages were 66.6% and 67.09%, with a 0.49% difference. Additionally, the penetration depth of the proton beam in soft tissue was 77 mm, while in the skull bone it was 55 mm, with only a 1mm difference from their equivalent TPU resins.

Therefore, the selected resins are deemed suitable for creating phantoms due to their availability and cost-effectiveness. The novelty of this researchlies in the careful design and selection of appropriate resin, enabling the creation of a phantom, using a new method. It is recommended to utilize 3D printers and newer materials for constructing such phantoms. The development of this phantom is part of our future plans, and the results will be presented in the upcoming investigations.

Conflict of interest

The authors declare no potential conflict of interest regarding the publication of this work.

References

[1] Shirazi SA, Pazirandeh A, Jahanfarnia G, Allaf MA. Presenting and simulating an innovative model of liver phantom and applying two methods for dosimetry of it in neutron radiation therapy. Reports of Practical Oncology & Radiotherapy. 2017 Jan 1;22(1):42-51.doi:10.1016/j.rpor.2016.09.013.

[2] Adam DP, Grudzinski JJ, Marsh IR, Hill PM, Cho SY, Bradshaw TJ, Longcor J, Burr A, Bruce JY, Harari PM, Bednarz BP. Voxel-Level Dosimetry for Combined Iodine 131 Radiopharmaceutical Therapy and External Beam Radiation Therapy Treatment Paradigms for Head and Neck Cancer. International Journal of Radiation Oncology* Biology* Physics. 2024 Jul 15;119(4):1275-84.doi: 10.1016/j.ijrobp.2024.02.005.

[3] Paduka S, Thongsawad S, Janthawanno P, Khaeongrod R, Ketphan K, Saiyo N. Assessment of organ doses from head and neck cone-beam computed tomography (CBCT) in adaptive radiation therapy: A phantom study. Radiation Physics and Chemistry. 2024 Feb 1;215:111338.doi: 10.1016/j.radphyschem.2023.111338.

[4] Büyükyıldız M, Kaur P, Thakur S, Atlı R. Study of phantom materials close to 1 keV photon energy for radiation applications. Radiation Physics and Chemistry. 2024 Feb 1;215:111375. doi: 10.1016/j.radphyschem.2023.111375.

[5] Zhang F, Zhang H, Zhao H, He Z, Shi L, He Y, Ju N, Rong Y, Qiu J. Design and fabrication of a

personalized anthropomorphic phantom using 3D printing and tissue equivalent materials. Quantitative imaging in medicine and surgery. 2019 Jan;9(1):94. doi: 10.21037/qims.2018.08.01.

[6] Mille MM, Griffin KT, Maass-Moreno R, Lee C. Fabrication of a pediatric torso phantom with multiple tissues represented using a dual nozzle thermoplastic 3D printer. Journal of Applied Clinical Medical Physics. 2020 Nov;21(11):226-36. doi:10.1002/acm2.13064.

[7] Okkalidis N. 3D printing methods for radiological anthropomorphic phantoms. Physics in Medicine & Biology. 2022 Jul 27;67(15):15TR04.doi: 10.1088/1361-6560/ac80e7

[8] Cederhag J, Kadesjö N, Nilsson M, Alstergren P, Shi XQ, Hellén-Halme K. Comparison of absorbed doses and organ doses measured with thermoluminescent dosimeters and Gafchromic film for cone beam computed tomography examination of the posterior mandibular region in a head phantom. Oral surgery, oral medicine, oral pathology and oral radiology. 2023 Dec 1;136(6):769-76. doi: 10.1016/j.oooo.2023.07.006.

[9] Iskanderani D, Nilsson M, Alstergren P, Hellén-Halme K. Dose distributions in adult and child head phantoms for panoramic and cone beam computed tomography imaging of the temporomandibular joint. Oral surgery, oral medicine, oral pathology and oral radiology. 2020 Aug 1;130(2):200-8.doi: 10.1016/j.oooo.2020.01.003

[10] Tran-Gia J, Schlögl S, Lassmann M. Design and fabrication of kidney phantoms for internal radiation dosimetry using 3D printing technology. Journal of Nuclear Medicine. 2016 Dec 1;57(12):1998-2005.doi: 10.2967/jnumed.116.178046

[11] Tino RB, Yeo AU, Brandt M, Leary M, Kron T. A customizable anthropomorphic phantom for dosimetric verification of 3D-printed lung, tissue, and bone density materials. Medical Physics. 2022 Jan;49(1):52-69.doi: 10.1002/mp.15364.

[12] Khatibani AB, Khoshhal AR, Tochaee EB, Jamnani SR, Moghaddam HM. Physical and gamma radiation shielding features of Sm2O3/graphene nanoparticles: A comparison between experimental and simulated gamma shielding capability. Inorganic Chemistry Communications. 2024 Jun 23:112772.doi: 10.1016/j.inoche.2024.112772.

[13] Khoshhal AR, Khatibani AB, Tirehdast Z, Shaddoust M, Nirouei M. Evaluation of experimental and simulated gamma ray shielding ability of ZnCo2O4 and ZnCo2O4/graphene nanoparticles. Optical Materials. 2024 Oct 1;156:115953.doi: 10.1016/j.optmat.2024.115953.

[14] Collaboration GE, Agostinelli S. GEANT4–a simulation toolkit. Nucl. Instrum. Meth. A. 2003 Jul;506(25):0.

[15] Hornbeck LJ. Digital light processing update: status and future applications. In Projection displays V 1999 May 20 (Vol. 3634, pp. 158-170). SPIE.doi: 10.1117/12.349351.

[16] Monk DW, Gale RO. The digital micromirror device for projection display. Microelectronic Engineering. 1995 Feb 1;27(1-4):489-93. doi: 10.1016/0167-9317(94)00151-J

[17] Chaudhary R, Fabbri P, Leoni E, Mazzanti F, Akbari R, Antonini C. Additive manufacturing by digital light processing: a review. Progress in Additive Manufacturing. 2023 Apr;8(2):331-51. doi: 10.1007/s40964-022-00336-0.

How to cite this article
A. R. Khoshhal*, A. Esmaili Torshabi, *Feasibility of Anthropomorphic Head Phantom Design Using DLP 3D Printing for Dosimetry*, Journal of Nuclear Research and Applications (JONRA) Volume 4 Number 3 Summer (2024) 24-32. **URL**: https://jonra.nstri.ir/article_1671.html, **DOI:** https://doi.org/10.24200/jonra.2024.1634.1140.